***General remarks***

*This is a well written paper that can be of interest for the hydrological modeling community using data assimilation. It presents the development and application of an adaptive inflation method specifically designed to counteract filter inbreeding in soil hydrology, when increasing the ensemble size is too computationally expensive. The method is applied and proved to work well in a small synthetic test case.*

*I used to think that inflation methods are not a good way to improve the ensemble Kalman filter, because in principle they are numerical tricks that, in my opinion, depart from the correct theory. When filter inbreeding occurs, the only mathematically consistent way to prevent it would be to increase the ensemble size, thus approaching the limit of an infinite ensemble for which the EnKF is demonstrated to converge to the Kalman filter. However, I recognize that in some cases this is not practically feasible and in this specific case I like the idea of an adaptive inflation factor that is estimated based on the difference between measurements and mean forecast state, i.e., based on physical considerations and that can give useful insights about the dynamics in the unsaturated zone.*

**Reply:** We thank the reviewer for the constructive comments and suggestions. We have revised our manuscript taking them into account. The difference pdf is attached and also includes the corrections based on the comments of referee #1. We reference (page, line) to this difference pdf.

We agree that inflation methods depart from the correct theory. To emphasize this we added (page 4, line 24) "heuristic" when introducing the multiplicative inflation.

*Other than relatively minor edits and comments, reported below, I think there is one main flaw in this paper: the method is demonstrated only in a fairly simple synthetic test case and it does not provide insights on possible issues in more realistic applications. I think an additional test case would make the paper more interesting and its conclusions more robust. The Authors themselves claim that the method has already been tested in a real-world application taken from Bauser et al. (2016): I strongly recommend that such an application be added to this paper and its results discussed in details.*

**Reply:** In the real world application described in Bauser et al. (2016), the EnKF is used to estimate the water content state, soil hydraulic parameters, Miller scaling factors and the upper boundary condition for a 1D representation of a soil profile at the Grenzhof test site close to Heidelberg, Germany, based on 11 TDR probes providing water content measurements. To account for uncertainties an assessment of all uncertainties for the specific situation is performed. In a three stage approach (improving the prior, standard EnKF, and closed-eye EnKF) the key uncertainties for this specific situation are reduced, except for an intermittent violation of the local equilibrium assumption in the Richards equation. These times were excluded from the parameter estimation to not incorporate the model error during this time into the parameters. Therefore the forecast during this time has larger errors and in this specific application especially the state inflation during the closed-eye period is important. Figure AC1 shows the inflation of the water content state in with the new inflation method. The main advantage of the new inflation in this case, is that (due to the fast adjustment) the inflation is mainly performed during the closed-eye period only and not continued afterwards.

Including this application into the paper, would increase the length of the paper considerably and require detailed explanations unrelated to the inflation method itself. However, we did not see any conceptually new insights from this application. Therefore, we do not want to include it in the paper, to keep it as concise as possible.

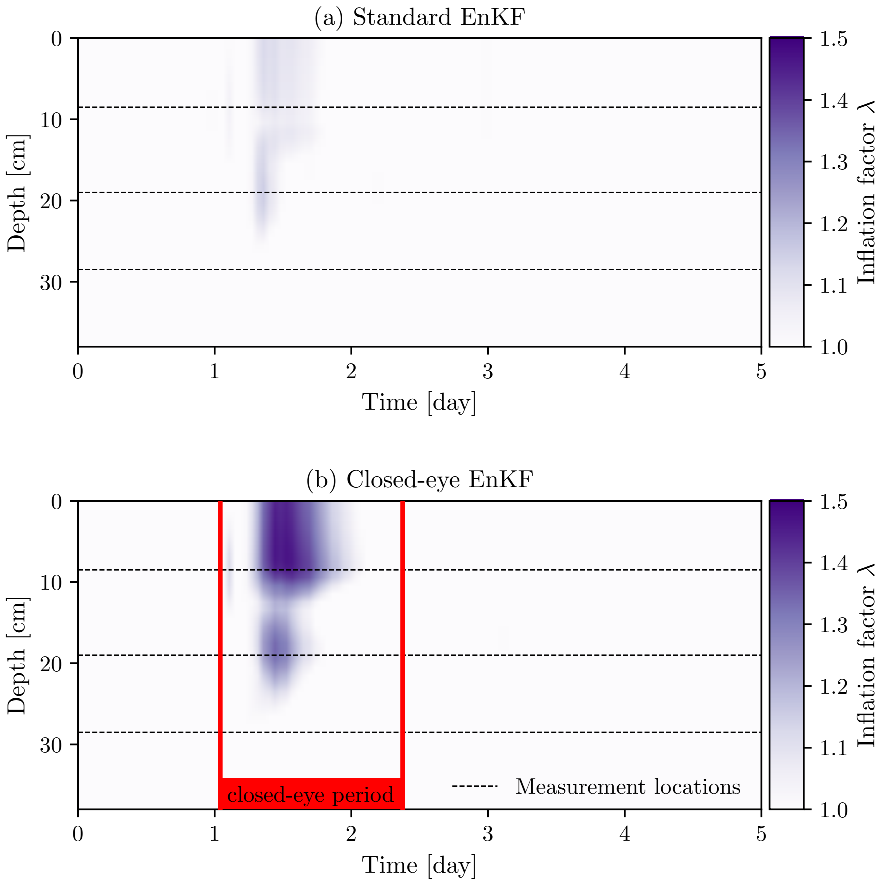


Figure AC1: Inflation factor $\lambda$ in the first layer during the last iteration of the standard EnKF and closed-eye EnKF. The covariance inflation increases the inflation factor around a measurement location when the deviations due to the infiltration reach the corresponding TDR. The deviations and consequently the inflation are stronger for the closed-eye EnKF, as the preferential flow is not incorporated into the parameters.

***Specific comments***

*Page 2, line 7: Another relevant reference is Botto et al. (2018) "Multi-source data assimilation for physically-based hydrological modeling of an experimental hillslop", still under discussion in HESS but already fully citable.*

**Reply:** We completely agree. Botto et al. (2018) must be citet. We became aware of the publication after submission of this manuscript. We included it in the introduction (page 2, line 7 and page 2, line 34).

*Page 3, Eq. 3: Strictly speaking, this is a scaled covariance matrix. The real one should be estimated dividing this by (N-1). Same for the matrix R in Eq. 4.*

**Reply:** Yes, we agree. However, we would like to follow the notation by Evensen (1994) and Burgers et al. (1998), where the overline generally denotes the expectation value. (We added this on page 3, line 28: "..., where the overline denotes the expectation value and $\overline{\boldsymbol{u}_k^{\mathrm{f}}}$ is the ensemble mean".) For the measurement error covariance matrix given in Eq. (4) we actually do not use the matrix calculated from the ensemble of measurement errors, but use the exact diagonal matrix with the measurement uncertainties. Therefore we prefer the more general expression.

*Page 5, lines 5-6: This statement requires an appropriate reference. Does it refer to a previous study by the same research group?*

**Reply:** To our knowledge there exists no study about the inflation method by Anderson (2009) applied to parameters. We are also not aware of an application of the method for parameter estimation in hydrology. Because of that, it is not our goal to perform an in depth analysis of the method. We cannot exclude that it might be possible to use the method, but in our tests, we could see possible over-inflation. Therefore we do not give a general statement in the paper but only state our experience ("However, we experienced possible over-inflation in parameters ..."). We would prefer to not work this out in the paper.

Below, we show results obtained with the inflation method by Anderson (2009) to support our statement. Like our proposed inflation, the inflation by Anderson (2009) can be used with a constant uncertainty $\sigma_\lambda$. The values are only roughly related to the values in our method though. Figures AC2, AC3 and AC4 show the results for different choices of $\sigma_\lambda$. They are all analogous to Fig. 3 in the manuscript. We also kept the same limits for the range of the axis for a better comparison.

Figure AC2 shows results for $\sigma_\lambda = 1$. Although the estimates for the mean values are excellent, the inflation is very strong. Especially the Miller scaling factor at 9.5 cm depth is inflated heavily and the good result is not guaranteed. This can be seen in Fig. AC3 ($\sigma_\lambda = 0.5$), where the inflation factor is adjusted slower. It still leads to very strong inflations for the Miller scaling factor at 9.5 cm depth and leads to wrong values in the hydraulic conductivity. Reducing the adjustment speed further (Fig. AC4, $\sigma_\lambda = 0.3$) leads to similar problems as in our inflation method: an overinflation of weakly correlated parameters for slow adjustment speeds.

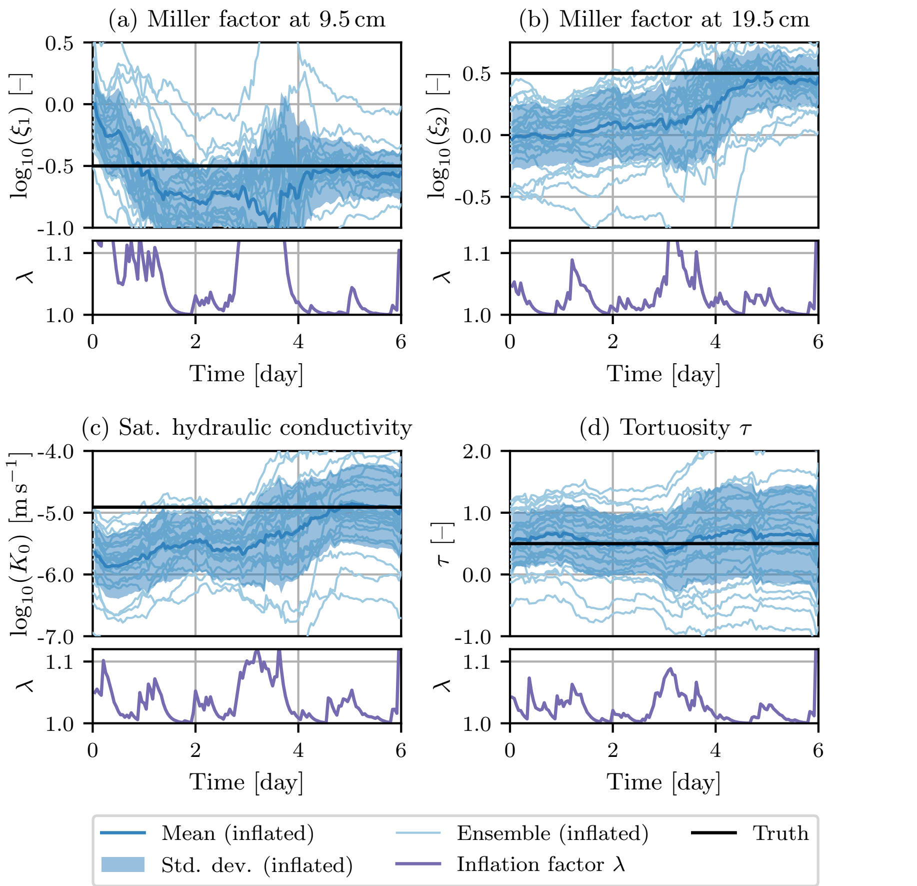


Figure AC2: Analogous to Figure 3, but with inflation method by Anderson (2009) and $\sigma_\lambda = 1$.

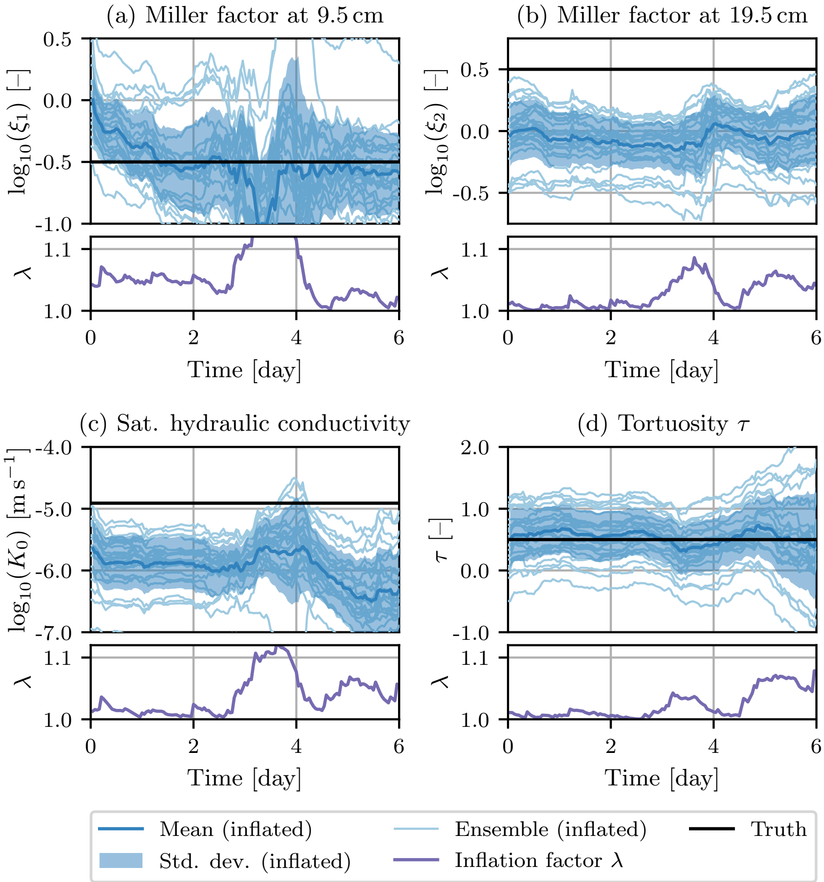


Figure AC3: Analogous to Figure 3, but with inflation method by Anderson (2009) and $\sigma_\lambda = 0.5$.

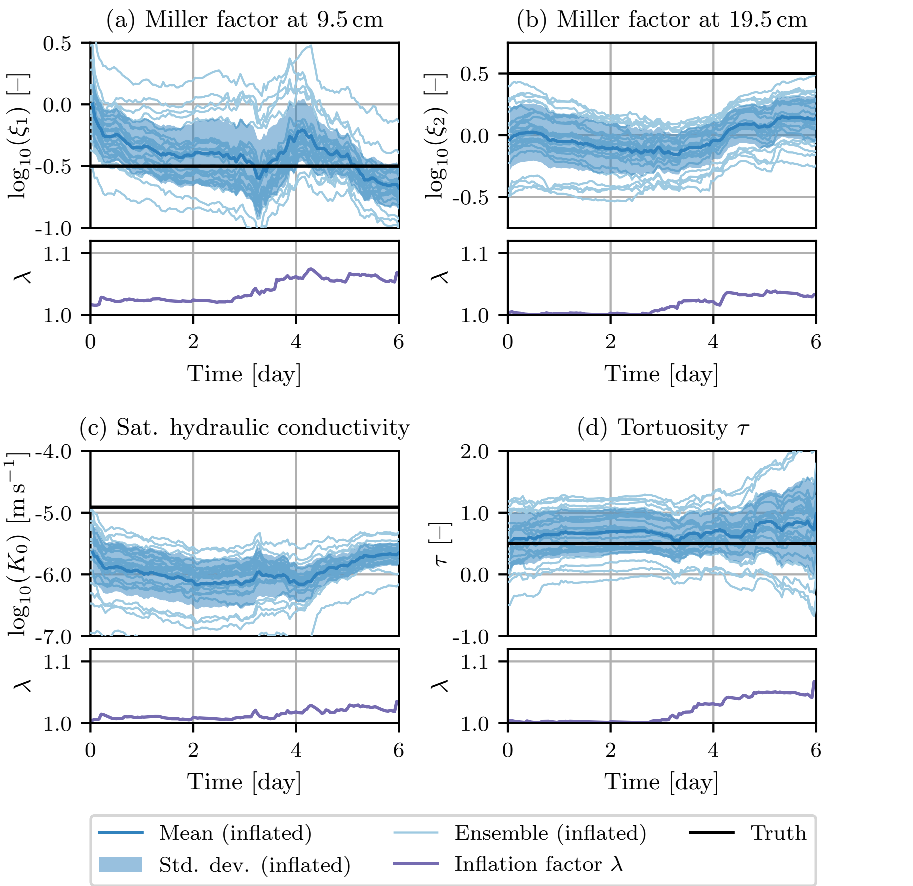


Figure AC4: Analogous to Figure 3, but with inflation method by Anderson (2009) and $\sigma_\lambda = 0.3$.

*Page 6, lines 18-19: This is a potentially important issue that is worth of further investigation. Why not repeating the analyses with one or two different values of the seed to actually show this sensitivity?*

**Reply:** Different behavior, because of the seed can be indeed an important issue. In this case it effects the behavior of the EnKF itself. The inflation method remains consistent with this behavior. Therefore, we do not want to include further seeds into the manuscript to keep it as concise as possible. We make our statement more clear and change it to (page 6, lines 21–23): "Due to a small ensemble size, the results vary depending on the seed of the random numbers. This however, is related to different performance of the EnKF itself. In simulations (results are not shown), we found that the behavior of the inflation remains consistent."

Figure AC5 shows the parameter estimation (analogous to Fig. 3 in the manuscript) for such a different seed. Especially the initial ensemble influences the correlations and consequently the corrections in the beginning. In this case, the Miller scaling factor at 19.5 cm has stronger correlations and is already corrected towards the true value. This leads to improved parameters at the beginning of the rain event. Therefore the inflation is larger in the beginning and smaller during the rain event.

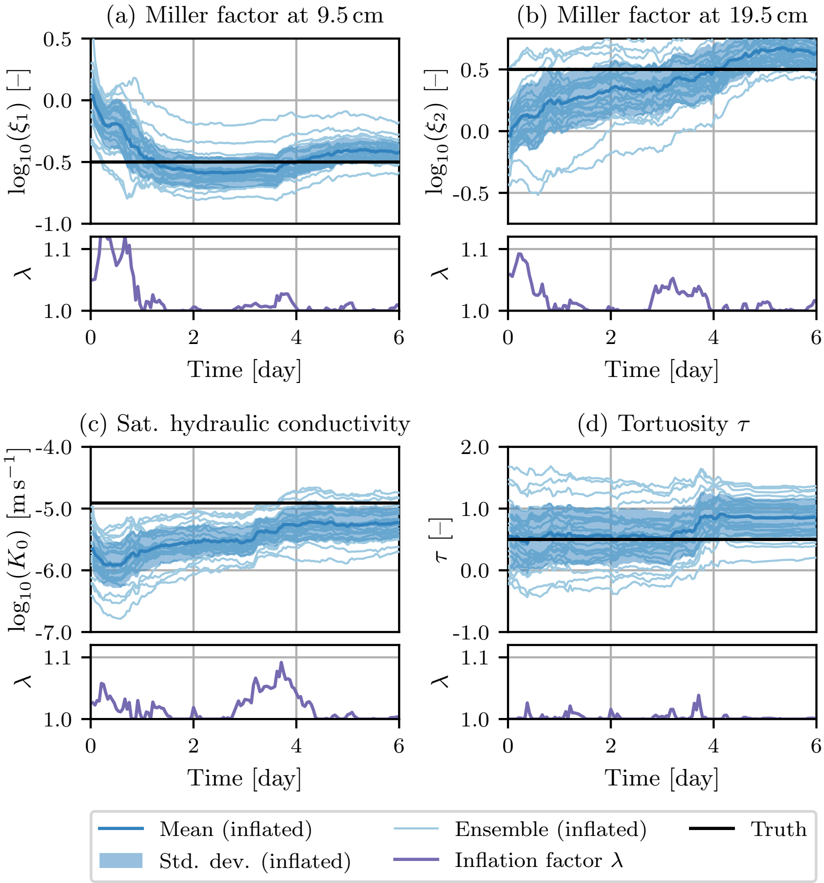


Figure AC5: Analogous to Figure 3, but with different seed.

*Page 7, lines 4-8: Please add appropriate reference and explain exactly how the spatial variability is taken into account. Is the parameter $\xi$ a function of space?*

**Reply:** Yes, it is. We added the Reference (Miller and Miller, 1956) and extended the explanation (page 7, lines 7–14) to "We additionally consider small scale heterogeneity through Miller scaling. It assumes geometrical similarity. With this the microscopic geometry of the pore space at a macroscopic position is parameterized by a single length scale $\xi$ and the macroscopic heterogeneity field can be generated with a single scalar field of this length scale. Miller and Miller (1956) showed that the hydraulic functions scale with this parameter according to

$$K(\theta) = K^*(\theta) \cdot \xi^2 \,, \tag{22}$$

$$h_\mathrm{m}(\theta) = h^*_\mathrm{m}(\theta) \cdot \frac{1}{\xi} \,, \tag{23}$$

where the functions $K(\theta)$ and $h_m(\theta)$ are defined at a reference point $^*$ with Miller scaling parameter $\xi = 1$ and from there are projected to all locations."

We additionally changed the explanation how the Miller scaling is included in the augmented state to (page 7, lines 22–24): "We reduce the description of the heterogeneity to these two parameters. The full function of the scaling factors is calculated by linearly interpolating between the measurement positions and constantly extrapolating to the boundaries."

*Page 10, lines 2-3: This statement is not clear. Can you please clarify, considering also the additional details required in the previous point?*

**Reply:** We extended the explanation to (page 8, lines 30–33): "This is due to the chosen interpolation of the Miller scaling factors. Through the interpolation between the measurement locations and extrapolation to the boundaries changes, the dynamics changes at the measurement locations. During the infiltration the dynamics is mainly influenced by the water content above and the correlations to these locations are stronger."

*Page 11, lines 28-30: As suggested above, this should be significantly expanded as a new section of the paper, where to show how the method works in a real-world application.*

**Reply:** Since the application to the real world case did not show any new conceptual insights, we did not include a new section here. Our goal is to keep the paper as concise as possible.

*Page 13, lines 8-12: Why would one want to use a multiplicative parameter in the boundary conditions? Maybe use a different example to illustrate this point.*

**Reply:** We see the boundary condition as a good example, where correlations could drop very rapidly. Different estimations of the boundary condition were included for example in Bauser et al. (2016) or Jaumann and Roth (2017). We agree that a multiplicative factor to the boundary condition is a very specific example. Therefore we generalize the statement to (page 13, lines 20–21): "An example could be a parameter only acting on an infiltration boundary condition."

*Page 13, lines 13-20: Similar to the previous one, also this paragraph is not very clear. Please rephrase and give practical examples of errors that can and cannot be represented with the augmented state.*

**Reply:** We rewrote the paragraph to (page 14, lines 3–15): "The method is in principle capable of compensating unrepresented model errors. However, it relies on correlations calculated from the forecast ensemble of the augmented state. If parameters have correlations to measurement locations with underestimated forecast uncertainties, the inflation will keep increasing the parameter spread until the forecast uncertainties are increased sufficiently. Therefore the correlations have to contain useful information. This means that inflating the parameters based on their correlations to measurement locations has to increase the forecast spread at these measurement locations. If the parameters have an insufficient influence on the state uncertainty an over-inflation of the parameters can occur. An example are measurements with underestimated measurement uncertainties and short time between measurements compared to the timescale of the dynamics. Then the parameters are not able to increase the state uncertainty in the short forecast time between measurements and the forecast dynamics is not able to represent the measurement noise. If such errors occur intermittently, e.g., the closed-eye period as proposed by Bauser et al. (2016) could be used to bridge these times. A rather heuristic solution could be a decay of the inflation factor towards values of 1, as already proposed by Anderson (2009)."

*Page 14, line 11: Please see previous point.*
**Reply:** We changed the sentence (analogous to the explanation above) to (page 14, lines 26–27): "The method requires that the correlations from in the forecast ensemble contain useful information for the inflation."

# Inflation Method for Ensemble Kalman Filter in Soil Hydrology

Hannes H. Bauser[1,2], Daniel Berg[1,2], Ole Klein[3], and Kurt Roth[1,3]

[1]Institute of Environmental Physics (IUP), Heidelberg University, Heidelberg
[2]HGS MathComp, Heidelberg University, Heidelberg
[3]Interdisciplinary Center for Scientific Computing (IWR), Heidelberg University, Heidelberg

*Correspondence to:* Hannes H. Bauser (hannes.bauser@iup.uni-heidelberg.de)

**Abstract.** The ensemble Kalman filter (EnKF) is a popular data assimilation method in soil hydrology. In this context, it is used to estimate states and parameters simultaneously. Due to unrepresented model errors and a limited ensemble size, state and parameter uncertainties can become too small during assimilation. Inflation methods are capable of increasing state uncertainties, but typically struggle with soil hydrologic applications. We propose a multiplicative inflation method specifically designed for the needs in soil hydrology. It employs a Kalman filter within the EnKF to estimate inflation factors based on the difference between measurements and mean forecast state within the EnKF. We demonstrate its capabilities on a small soil hydrologic test case. The method is capable of adjusting inflation factors to spatiotemporally varying model errors. It successfully transfers the inflation to parameters in the augmented state, which leads to an improved estimation.

## 1 Introduction

Data assimilation combines information from models and measurements into an optimal estimate of a geophysical field of interest (Reichle, 2008). It has applications in all branches of the geosciences, with weather forecasting as the driving force behind many recent advances (van Leeuwen et al., 2015). The advantage of data assimilation methods (in contrast to e.g. inverse modeling) is the possibility to consider model errors, which are characteristic for geophysical systems.

The ensemble Kalman filter (EnKF) (Evensen, 1994; Burgers et al., 1998) is a popular data assimilation method due to its simple conceptional formulation and ease of implementation (Evensen, 2003). It is an extension of the Kalman filter (Kalman, 1960) for nonlinear models.

In hydrology, the EnKF was used for soil moisture estimation from satellite data (e.g. Reichle et al., 2002; Crow and Van Loon, 2006) or from local measurements (e.g. De Lannoy et al., 2007, 2009; Camporese et al., 2009). However, the largest uncertainties in hydrology are associated with soil hydraulic material properties. They can neither be measured directly, nor can they be transferred from the lab to the field, and are typically parameterized. Thus, including material properties into the estimation can be crucial in hydrology. Liu and Gupta (2007) called for an integrated assimilation framework including not only states but parameters, and even model structure.

The joint estimation of states and parameters in data assimilation might be one possibility to reduce the influence of model errors on parameter estimation (Liu et al., 2012). Such a joint estimation in the EnKF with an augmented state was already demonstrated by Anderson (2001) for an atmospheric model. In hydrology Vrugt et al. (2005) combined an EnKF and the shuffled complex evolution Metropolis algorithm, while Moradkhani et al. (2005) used a dual EnKF approach to estimate states and parameters for a rainfall-runoff model. The joint assimilation of states and parameters in an augmented state was successfully performed for example in groundwater research (e.g. Chen and Zhang, 2006; Hendricks Franssen and Kinzelbach, 2008; Kurtz et al., 2012, 2014; Erdal and Cirpka, 2016), but also in soil hydrology for land surface models (e.g. Bateni and Entekhabi, 2012; Han et al., 2014; Zhang et al., 2017) and on smaller scales based on the Richards equation (e.g. Li and Ren, 2011; Wu and Margulis, 2011, 2013; Song et al., 2014; Erdal et al., 2014, 2015; Shi et al., 2015; Bauser et al., 2016)(Botto et al., 2018).

Due to unrepresented model errors and due to a limited ensemble size, the EnKF underestimates model errors, which can lead to filter inbreeding. Systematic model errors are common for example in land surface models (Vereecken et al., 2015). Additionally, in soil hydrology spatially and temporally varying model errors occur due to un- or ill-represented processes like preferential flow or hysteresis. Underestimated errors cause an insufficient ensemble spread in the augmented state. This is especially severe for parameters, which are typically not changed through a forward propagation and consequently cannot increase their uncertainty again. Due to the convergent dynamics in soil hydrology, the uncertainty in the state depends strongly on the parameter spread and becomes too small as well.

Covariance inflation can counteract filter inbreeding. Different methods have been proposed: (i) Additive inflation, which adds a model error after the forward propagation. This method is especially useful if prior knowledge about the model error exists. In atmospheric sciences additive inflation has been successfully applied by e.g. using reanalysis of historical weather prediction errors (Whitaker et al., 2008). (ii) Relaxation methods, which relax the analysis back to a prior perturbation or spread, have been proposed with tuning parameters (Zhang et al., 2004; Whitaker and Hamill, 2012) or based on deviations to measurements (Ying and Zhang, 2015). (iii) Multiplicative covariance inflation, which inflates the complete state with a scalar factor, where the inflation factor is either chosen manually (Anderson and Anderson, 1999) or is estimated based on deviations from measurements (e.g. Wang and Bishop, 2003; Anderson, 2007; Li et al., 2009). This method has been further extended to inflate each state component individually (Anderson, 2009).

All these inflation methods are developed in an atmospheric sciences context. Their transfer to soil hydrology is limited, due to the spatiotemporally varying model errors and the typically employed augmented state. For groundwater research, Kurtz et al. (2012) reported improved results by employing the inflation method by Anderson (2007), and Kurtz et al. (2014) used the constant inflation by Anderson and Anderson (1999). In soil hydrology, however, adjusted methods have been used: For example Han et al. (2014) and Zhang et al. (2017) apply a special case of the inflation method by Whitaker and Hamill (2012) and keep the parameter spread constant to ensure a sufficient ensemble spread. Bauser et al. (2016) used the method by Anderson (2009), but adjusted the inflation of parameters.

Alternatively, no inflation method is reported (e.g. Li and Ren, 2011; Shi et al., 2015), but instead a damping factor (Hendricks Franssen and Kinzelbach, 2008), which can alleviate the issue, is employed. This is done by e.g. Wu and Margulis (2011); Song et al. (2014); Erdal et al. (2014); Brandhorst et al. (2017); Botto et al. (2018), where Erdal et al. (2014) and Brandhorst et al. (2017) combined this method with additive inflation.

In this paper, we propose a novel multiplicative inflation method, specifically designed for the needs in the soil hydrology community. The inflation method can vary rapidly in space and time to cope with the typically varying model errors and it is capable of a transfer of the inflation in the state to the parameters in the augmented state. The remainder of this paper is organized as follows: Sect. 2 describes (i) the EnKF, (ii) our proposed inflation method and (iii) a soil hydrologic test case. Section 3 shows the results of our method applied to the test case, followed by discussion and conclusion in Sect. 4 and 5.

## 2 Method

### 2.1 Ensemble Kalman Filter

The EnKF (Evensen, 1994; Burgers et al., 1998) is the Monte Carlo extension of the Kalman filter (Kalman, 1960) for nonlinear models and assumes unbiased Gaussian error distributions to combine model and measurement information. The filter is a sequential method and alternates between a forecast step and an analysis step. The forecast propagates a state including its uncertainty forward in time. The analysis combines uncertain model information with uncertain measurements at this time into an optimal estimate of the state. These two steps are now explained in more detail.

The forecast propagates an ensemble of states $\boldsymbol{\varphi}^n$ forward from time $k-1$ to time $k$ with a model $M$,

$$\boldsymbol{\varphi}_k^{\mathrm{f},n} = M(\boldsymbol{\varphi}_{k-1}^{\mathrm{a},n}) + \boldsymbol{\beta}^n\,, \tag{1}$$

where the superscripts f and a denote forecast and analysis respectively, while $n$ denotes the ensemble members with $n = 1,...,N$. The uncertainty in the state is directly represented through the ensemble $\boldsymbol{\varphi}_{k-1}^{\mathrm{a},n}$ and then propagated nonlinearly with the model. Unrepresented model errors can be added through the unbiased Gaussian process noise $\boldsymbol{\beta}$. This is also called additive inflation. However, the details of the model error are typically unknown and thus not represented adequately. The propagated uncertainties are directly represented through the new forecast ensemble $\boldsymbol{\varphi}_k^{\mathrm{f},n}$.

The state can be extended by e.g. model parameters $\boldsymbol{\phi}$ to an augmented state $\boldsymbol{u} = [\boldsymbol{\varphi}, \boldsymbol{\phi}]$. This requires a forecast for each augmented state component. Parameters are typically assumed to be constant in time:

$$\boldsymbol{\phi}_k^{\mathrm{f},n} = \boldsymbol{\phi}_{k-1}^{\mathrm{a},n}\,. \tag{2}$$

The forecast of the state $\boldsymbol{\varphi}_k^{\mathrm{f},n}$ now also depends on the corresponding parameter set $\boldsymbol{\phi}_{k-1}^{\mathrm{a},n}$. This way, uncertainties in the parameters are propagated as well and can be reduced jointly in the analysis.

Assuming unbiased Gaussian distributions, the ensemble of augmented states is characterized through the forecast error covariance matrix $\mathbf{P}^{\mathrm{f}}$,

$$\mathbf{P}_k^{\mathrm{f}} = \overline{\left[\boldsymbol{u}_k^{\mathrm{f},n} - \overline{\boldsymbol{u}_k^{\mathrm{f}}}\right]\left[\boldsymbol{u}_k^{\mathrm{f},n} - \overline{\boldsymbol{u}_k^{\mathrm{f}}}\right]^T}\,, \tag{3}$$

where the ~~ensemble mean $\overline{\boldsymbol{u}_k^{\mathrm{f}}}$ denotes the best guess~~overline denotes the expectation value and $\overline{\boldsymbol{u}_k^{\mathrm{f}}}$ is the ensemble mean.

The analysis combines model and measurement information based on the Gaussian error assumption. The measurement error covariance matrix $\mathbf{R}$ of the measurements $\boldsymbol{d}$ is defined analogously as

$$\mathbf{R}_k = \overline{[\boldsymbol{\epsilon}_k^n]\,[\boldsymbol{\epsilon}_k^n]^T}\,, \tag{4}$$

where $\boldsymbol{\epsilon}$ is the measurement error. The measurements are linked to the state through the linear measurement operator $\mathbf{H}$, which maps from the state space to the measurement space:

$$\boldsymbol{d}_k = \mathbf{H}_k \boldsymbol{u}_{\text{true},k} + \boldsymbol{\epsilon}_k\,. \tag{5}$$

The Kalman gain $\mathbf{K}$ weighs the forecast error covariance matrix with the measurement error covariance matrix and maps from the measurement space back to the state space, based on the covariances in the forecast error covariance matrix:

$$\mathbf{K}_k = \mathbf{P}_k^{\text{f}} \mathbf{H}_k^T \left[\mathbf{H}_k \mathbf{P}_k^{\text{f}} \mathbf{H}_k^T + \mathbf{R}_k\right]^{-1}. \tag{6}$$

~~The Kalman gain is used to update~~ Based on the measurements, the Kalman gain updates the forecast ensemble ~~based on the measurements~~ to the analysis ensemble:

$$\boldsymbol{u}_k^{\text{a},n} = \boldsymbol{u}_k^{\text{f},n} + \mathbf{K}_k \left[\boldsymbol{d}_k + \boldsymbol{\epsilon}_k^n - \mathbf{H}_k \boldsymbol{u}_k^{\text{f},n}\right]. \tag{7}$$

This update to the ensemble $\boldsymbol{u}_k^{\text{a},n}$ minimizes the analysis error covariance $\mathbf{P}_k^a$, which fulfills

$$\mathbf{P}_k^{\text{a}} = \left[\mathbf{I} - \mathbf{K}_k \mathbf{H}_k\right] \mathbf{P}_k^{\text{f}}\,, \tag{8}$$

for infinite ensemble sizes.

Through spurious correlations and non-Gaussian distributions, $\mathbf{P}_k^{\text{a}}$ will become too small, which can lead to filter inbreeding and ultimately filter divergence (e.g. Hamill et al., 2001). This is intensified, if the model error required in Eq. (1) is unknown.

A common way to alleviate this issue in hydrology is the use of a damping factor $\gamma \in [0,1]$ (Hendricks Franssen and Kinzelbach, 2008), which is multiplied to the correction vector in Eq. (7) and consequently lessens the uncertainty reduction. The damping factor can be extended to a vector $\boldsymbol{\gamma}$ (and an entrywise multiplication) to treat augmented state components differently (Wu and Margulis, 2011). Typically, parameters are multiplied with a smaller factor than the state. However, the damping factor can only alleviate and not completely prevent the inbreeding problem.

### 2.2 Multiplicative inflation for soil hydrology

Multiplicative inflation is another heuristic way to avoid filter inbreeding. Anderson and Anderson (1999) proposed to increase the distance of each ensemble member to the ensemble mean by multiplying this distance by $\sqrt{\lambda}$ for the inflation factor $\lambda \geq 1$:

$$\boldsymbol{u}_{\text{inf}}^{\text{f},n} = \sqrt{\lambda}\left(\boldsymbol{u}^{\text{f},n} - \overline{\boldsymbol{u}^{\text{f}}}\right) + \overline{\boldsymbol{u}^{\text{f}}}\,. \tag{9}$$

This inflation factor is applied to the complete augmented state and has to be adjusted to the specific problem. By construction, it does not alter the mean value: $\overline{\boldsymbol{u}^{\mathrm{f}}_{\mathrm{inf}}} = \overline{\boldsymbol{u}^{\mathrm{f}}}$. A temporally varying inflation factor can be estimated by comparing uncertainties with the distance of measurement and forecast (e.g. Wang and Bishop, 2003; Anderson, 2007; Li et al., 2009). A spatiotemporally adaptive inflation has been achieved by estimating a vector $\boldsymbol{\lambda}$ for the complete augmented state (Anderson, 2009). The author uses the correlation between measurements and augmented state dimensions and asks the question: *How much inflation is required in each dimension to explain the observed differences to the measurements?* Anderson (2009) showed that this works excellently for the actual state. However, we experienced possible over-inflation in parameters (which do not have any dynamics to compensate for this), which can lead to filter collapses.

We propose a more conservative inflation method and ask the question: *How much of the required change of the inflation are we allowed to transfer to the state dimensions based on the correlation information?* This can be achieved by applying a Kalman filter for the inflation within the EnKF.

In this Kalman filter, the inflation vector is treated as the state variable. As for parameters, we choose a constant model for the forecast in time:

$$\boldsymbol{\lambda}^{\mathrm{f}}_{k} = \boldsymbol{\lambda}^{\mathrm{a}}_{k-1}\,. \tag{10}$$

For convenience we will drop the time subscript $k$ in the following. Furthermore, we will use the same symbols as for the EnKF, but denote them with the subscript $\lambda$. We approximate the forecast error covariance matrix for lambda, $\mathbf{P}^{\mathrm{f}}_{\lambda}$, based on the covariance matrix of the augmented state in the EnKF, $\mathbf{P}^{\mathrm{f}}$, as the normalized absolute correlation matrix of the augmented state ensemble. The matrix component $ij$ is determined as

$$\left(\mathbf{P}^{\mathrm{f}}_{\lambda}\right)_{ij} = \sigma^2_{\lambda} \left|\left(\mathbf{P}^{\mathrm{f}}\right)_{ij}\right| \left[\left(\mathbf{P}^{\mathrm{f}}\right)_{ii}\left(\mathbf{P}^{\mathrm{f}}\right)_{jj}\right]^{-\frac{1}{2}}, \tag{11}$$

where ~~$\sigma^2_{\lambda}$~~ $\sigma_{\lambda}$ denotes the uncertainty of the inflation factors. It is a tuning parameter that is kept constant over time and is assigned to all state dimensions. It influences how fast the inflation factors are adjusted. This follows the idea by Anderson (2007, 2009) to avoid a closure problem, where the inflation estimation would require its own inflation. Instead, the uncertainty is kept constant. Furthermore, only the absolute value of the correlation is considered, since the inflation is based on differences between measurement and model, but ignores their direction. Note, that this presumes that the correlations of the model state can be transferred to the inflation. In the presence of unknown model errors this assumption may or may not be correct. However, the estimation at measurement locations will remain meaningful in any case.

For the analysis, the distance $\boldsymbol{d}_{\lambda}$ between mean forecast and measurement is used as measurement for $\boldsymbol{\lambda}$:

$$\boldsymbol{d}_{\lambda} = \left|\boldsymbol{d} - \mathbf{H}\overline{\boldsymbol{u}^{\mathrm{f}}_{\mathrm{inf}}}\right|. \tag{12}$$

The measurement error covariance matrix $\mathbf{R}_{\lambda}$ of $\boldsymbol{d}_{\lambda}$ can be calculated based on the error covariance matrices of $\boldsymbol{d}$ and $\mathbf{H}\overline{\boldsymbol{u}^{\mathrm{f}}_{\mathrm{inf}}}$,

$$\left(\mathbf{R}_{\lambda}\right)_{ij} = \left|\left(\mathbf{R}\right)_{ij} + \left(\mathbf{H}\mathbf{P}^{\mathrm{f} \circ \sqrt{\boldsymbol{\lambda}^{\mathrm{f}}}\sqrt{\boldsymbol{\lambda}^{\mathrm{f}}}^{T}}_{\mathrm{inf}}{}^{\mathrm{f}}\mathbf{H}^{T}\right)_{ij}\right|, \tag{13}$$

where the current inflation $\boldsymbol{\lambda}^{\mathrm{f}}$ is already considered. inflated forecast error covariance matrix $\mathbf{P}^{\mathrm{f}}_{\mathrm{inf}}$ can be calculated from the inflation vector and the forecast error covariance matrix by combining Eq. (9) (with vector lambda and entrywise multiplication) and Eq. (3): $\mathbf{P}^{\mathrm{f}}_{\mathrm{inf}} = \mathbf{P}^{\mathrm{f}} \circ [\sqrt{\boldsymbol{\lambda}^{\mathrm{f}}}\sqrt{\boldsymbol{\lambda}^{\mathrm{f}}}^T]$. The entrywise product is denoted by $\circ$ and the entrywise square root of $\boldsymbol{\lambda}$ by $\sqrt{\boldsymbol{\lambda}}$.

The expected distance between measurement and mean forecast based on the current inflation is

$$\left(\boldsymbol{h}_\lambda(\boldsymbol{\lambda}^{\mathrm{f}})\right)_i = \left[(\mathbf{R}_\lambda)_{ii}\right]^{\frac{1}{2}} , \tag{13}$$

which combines the uncertainties of $\boldsymbol{d}$ and $\mathbf{H}\overline{\boldsymbol{u}^{\mathrm{f}}_{\mathrm{inf}}}$. To be able to determine the Kalman gain, we first calculate the Jacobian matrix $\mathbf{H}_\lambda$ of partial derivatives of $\boldsymbol{h}_\lambda$ with respect to $\boldsymbol{\lambda}$:

$$(\mathbf{H}_\lambda)_{ij} = \frac{\partial}{\partial\left(\boldsymbol{\lambda}^{\mathrm{f}}\right)_j}\left(\boldsymbol{h}_\lambda(\boldsymbol{\lambda}^{\mathrm{f}})\right)_i , \tag{14}$$

$$= \left[2\left[(\boldsymbol{\lambda}^{\mathrm{f}})_j\right]^{\frac{1}{2}}\left(\boldsymbol{h}_\lambda(\boldsymbol{\lambda}^{\mathrm{f}})\right)_i\right]^{-1}\sum_m (\mathbf{H})_{ij}(\mathbf{H})_{im}(\mathbf{P}^{\mathrm{f}})_{jm}\left[\left(\boldsymbol{\lambda}^{\mathrm{f}}\right)_m\right]^{\frac{1}{2}} . \tag{15}$$

With this approximated measurement operator $\mathbf{H}_\lambda$, the Kalman gain $\mathbf{K}_\lambda$ and the analysis state $\boldsymbol{\lambda}^{\mathrm{a}}$ are obtained as

$$\mathbf{K}_\lambda = \mathbf{P}^{\mathrm{f}}_\lambda \mathbf{H}^T_\lambda\left[\mathbf{H}_\lambda \mathbf{P}^{\mathrm{f}}_\lambda \mathbf{H}^T_\lambda + \mathbf{R}_\lambda\right]^{-1} , \tag{16}$$

$$\boldsymbol{\lambda}^{\mathrm{a}} = \boldsymbol{\lambda}^{\mathrm{f}} + \mathbf{K}_\lambda\left[\boldsymbol{d}_\lambda - \boldsymbol{h}_\lambda(\boldsymbol{\lambda}^{\mathrm{f}})\right] . \tag{17}$$

Note, that the matrices $\mathbf{P}^{\mathrm{f}}_\lambda$ and $\mathbf{R}_\lambda$ can possibly become indefinite, due to the absolute value in Eq. (11) and Eq. (13). Consequently, the inverse in Eq. (16) could become unfeasible. However, we never encountered such a case. In a situation with uncorrelated measurements, the issue can be resolved by reducing $\sigma^2_\lambda$ $\sigma_\lambda$ just for that single time step.

With this Kalman filter, the inflation vector is updated at each time step based on the difference of the mean forecast to the measurements. Following Anderson (2007), we additionally prohibit a deflation by constraining the inflation values to $(\boldsymbol{\lambda})_i \geq 1$.

### 2.3 Model

We test the proposed inflation method on a small hydrologic test case. We constructed it specifically to require a strong inflation. This makes it possible to explore features of the inflation in detail on a rather short timescale. Due to a small ensemble size, the results will also vary depending on the seed of the random numbers. This however, is related to different performance of the EnKF itself. In simulations (results are not shown), we found that the behavior of the inflation remains consistent.

The Richards equation describes the change of volumetric soil water content $\theta$ (–) in a continuous porous medium,

$$\frac{\partial\theta}{\partial t} - \nabla\cdot\left[K(\theta)\left[\nabla h_{\mathrm{m}}(\theta) - 1\right]\right] = 0 , \tag{18}$$

where $K$ (L T$^{-1}$) is the isotropic conductivity and $h_{\mathrm{m}}$ (L) is the matric head. Both are related to the water content. This relation is typically described through parameterized material properties. We choose the Mualem–van Genuchten parameterization

(Mualem, 1976; van Genuchten, 1980),

$$K(\Theta) = K_0 \Theta^\tau \left[1 - \left[1 - \Theta^{n/[n-1]}\right]^{1-1/n}\right]^2 , \tag{19}$$

$$h_m(\Theta) = \frac{1}{\alpha}\left[\Theta^{-n/[n-1]} - 1\right]^{1/n} , \tag{20}$$

with the saturation $\Theta$ (–),

$$\Theta := \frac{\theta - \theta_\mathrm{r}}{\theta_\mathrm{s} - \theta_\mathrm{r}} . \tag{21}$$

The parameterization is described by a set of six parameters: $\theta_\mathrm{s}$ (–), $\theta_\mathrm{r}$ (–), $\alpha$ ($\mathrm{L}^{-1}$), $n$ (–), $K_0$ ($\mathrm{L\,T}^{-1}$) and $\tau$ (–).

We additionally consider small scale heterogeneity through Miller scaling. It assumes geometrical similarity~~and scales the material properties at each location according to ,~~. With this the microscopic geometry of the pore space at a macroscopic position is parameterized by a single length scale $\xi$ and the macroscopic heterogeneity field can be generated with a single scalar field of this length scale. Miller and Miller (1956) showed that the hydraulic functions scale with this parameter according to

$$K(\theta) = K^*(\theta) \cdot \xi^2 , \tag{22}$$

$$h_\mathrm{m}(\theta) = h^*_\mathrm{m}(\theta) \cdot \frac{1}{\xi} , \tag{23}$$

where the functions $K(\theta)$ and $h_m(\theta)$ are defined at a reference point $^*$ ~~denotes the reference material properties and $\xi$ (–) is the spatially varying~~ with Miller scaling parameter $\xi = 1$ and from there are projected to all locations.

For the test, we choose a one-dimensional case with a depth of 50 cm for a time of 6 days. We set a groundwater table as the lower boundary condition throughout the whole time and start from equilibrium conditions. The upper boundary condition is no flux, except for a rain event with $2.0{\cdot}10^{-7}$ [$\mathrm{m\,s}^{-1}$] during the fourth day. As observations we choose two water content measurements at a depth of 9.5 cm and 19.5 cm as they would be available from time domain reflectometry (TDR). We set the measurement uncertainty to a standard deviation of 0.007 (e.g. Jaumann and Roth, 2017).

As material we choose sandy loam from Carsel and Parrish (1988): $\theta_\mathrm{s} = 0.41$, $\theta_\mathrm{r} = 0.065$, $\alpha = -7.5\,\mathrm{m}^{-1}$, $n = 1.89$, $K_0 = 1.23{\cdot}10^{-5}\,\mathrm{m\,s}^{-1}$ and $\tau = 0.5$. For the Miller scaling we choose $\xi_1 = 0.32$ at the upper measurement position and $\xi_2 = 3.2$ at the lower measurement position. ~~The scaling factors are linearly interpolated~~ We reduce the description of the heterogeneity to these two parameters. The full function of the scaling factors is calculated by linearly interpolating between the measurement positions and constantly ~~extrapolated~~ extrapolating to the boundaries.

The forward simulations are performed using MuPhi (Ippisch et al., 2006) with a spatial resolution of 1 cm. This corresponds to a state with 50 dimensions.

To test the inflation method, we perform a perfect model experiment. With the EnKF we estimate the water content state and four parameters ($\xi_1$, $\xi_2$, $K_0$ and $\tau$) through the augmented state $\boldsymbol{u} = [\boldsymbol{\theta}, \log_{10}(\xi_1), \log_{10}(\xi_2), \log_{10}(K_0), \tau]$. We choose to include the logarithm of $\xi_1$, $\xi_2$ and $K_0$, because we expect a more linear relation to the water content state, than for the actual parameters. For the water content state, we use the correct initial condition as the mean with an uncertainty of 0.005. The uncertainty is spatially correlated using the fifth-order piecewise rational function by Gaspari and Cohn (1999) with the length-scale $c = 5$ cm. As initial guess for the parameters, we start with unknown heterogeneity $\log_{10}(\xi_1) = \log_{10}(\xi_2) = 0.0 \pm 0.25$, corresponding to two standard deviations away from the true values of $\log_{10}(\xi_1) = -0.5$ and $\log_{10}(\xi_2) = 0.5$. For the saturated hydraulic conductivity, we choose a too small value of $\log_{10}(K_0) = -5.5 \pm 0.5$, $K_0$ in $(\mathrm{m\,s^{-1}})$, which is about one standard deviation away from the true value of $\log_{10}(K_0) = -4.9$. For the tortuosity $\tau = 0.5 \pm 0.5$ we start from the true value.

Through the unrepresented heterogeneity, we can mimic a model error, leading to a bias towards smaller values for the estimation of $K_0$ during times without dynamics, which may necessitate inflation. The parameter $\tau$ is expected to have a smaller influence, since the uncertainty is chosen small and it is already at the true value. This way it can act as an indicator parameter for the inflation as it does not require inflation.

The EnKF is set up with a total of 25 ensemble members and a damping vector of $\boldsymbol{\gamma} = [\mathbf{1.0}, 0.3, 0.3, 0.3, 0.3]$, which we also apply to the inflation. The damping factor of 0.3 is applied to the parameters to alleviate issues of nonlinear relations between observations and parameters. For the uncertainty of the inflation factors we choose ~~$\sigma_\lambda^2 =$~~ $\sigma_\lambda =$ 1.0.

## 3 Results

We estimate the water content state together with the four parameters $\xi_1$, $\xi_2$, $K_0$ and $\tau$ with the EnKF as described in Sect. 2.3. The development of the water content at the two measurement locations at a depth of 9.5 cm and 19.5 cm is shown together with the inflation factor at these locations in Fig. 1. The inflation factor is applied to the forecast ensemble before the analysis. The standard deviation of the inflated ensemble should describe the distance of the estimated mean to the synthetic truth. Note, that the inflation factor is not based on this distance and relies on the noisy measurements. Therefore, it is only an indicator.

During the first three days without any dynamics, the uncertainty for the upper measurement is slightly underestimated, while the uncertainty in the lower measurement is slightly overestimated. This leads to an inflation factor of basically 1 for the lower measurement (factors smaller than 1 are not allowed), while the inflation factor for the upper measurement is larger. However, due to correlations between the measurement locations a stronger inflation to fully explain the difference to the truth is prevented.

The deviation from the synthetic truth is induced through the initial guess of no heterogeneity and can also be seen in the systematic deviation of the inflated mean (which is equal to the forecast mean) from the analysis mean. When the infiltration front reaches the measurements, the deviations from the truth, underestimation of the uncertainty, and inflation factors increase rapidly. All of them are more pronounced for the upper measurement location. After the main peak, the differences and also the inflation factors decrease rapidly again.

The inflation factor for the state is shown in Fig. 2. It shows the strong increase of the inflation factor during the infiltration and its fast decrease afterwards. The inflation is strongest at the measurement location at a depth of 9.5 cm. The inflation factor is transferred to the other state locations through the correlations, which decrease with distance. Directly below the measurement locations the inflation factors are increased less than above. This is due to the chosen interpolation of the Miller scaling ~~factor, which reduces the correlations from~~ factors. Through the interpolation between the measurement locations and extrapolation to the boundaries changes, the dynamics changes at the measurement locations~~to these state locations .~~. During the infiltration the dynamics is mainly influenced by the water content above and the correlations to these locations are stronger.

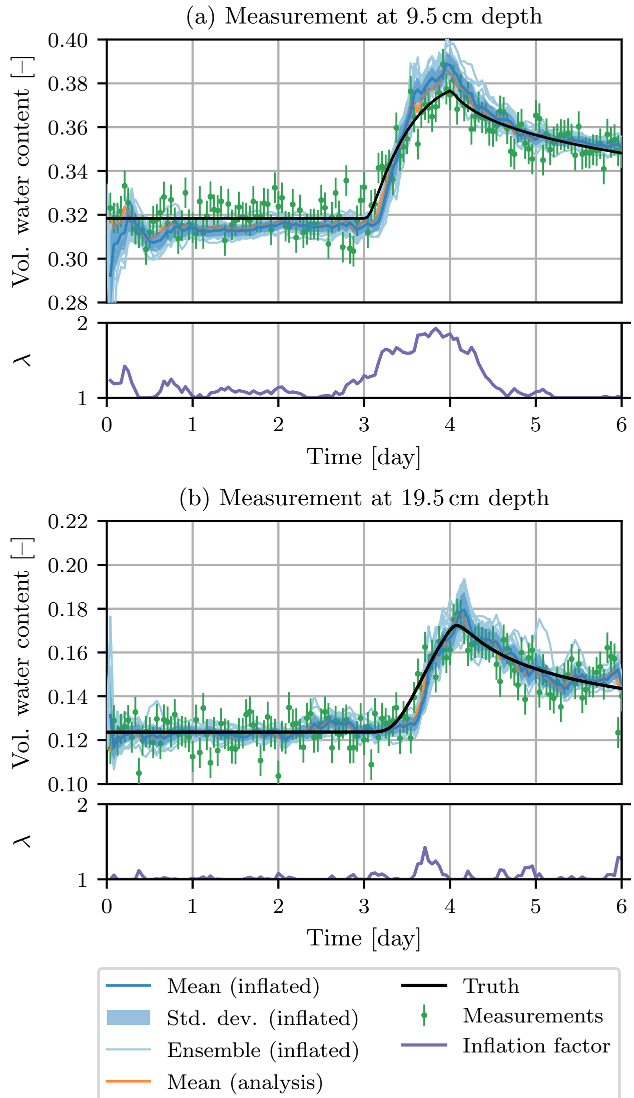


**Figure 1.** Water content estimation at the two measurement locations. The standard deviation of the inflated ensemble should be able to explain the differences between the inflated mean and the synthetic truth. The inflation factor is increased, when the ensemble uncertainty is too small.

The development of the Miller scaling factors $\xi_1$ and $\xi_2$ at the two measurement positions (9.5 cm and 19.5 cm depth) is shown in Fig. 3(a) and 3(b) together with the estimated inflation factor for these parameters. Both initial conditions assume no heterogeneity and start at $\log_{10}(\xi_1) = \log_{10}(\xi_2) = 0.0 \pm 0.25$, corresponding to two standard deviations away from the true value. At the upper location the true value of $\log_{10}(\xi_1) = -0.5$ corresponds to a finer material. Consequently, the water content drops, as seen in Fig. 1, leading to a strong correlation with the scaling factor, and $\log_{10}(\xi_1)$ is adjusted rapidly to lower

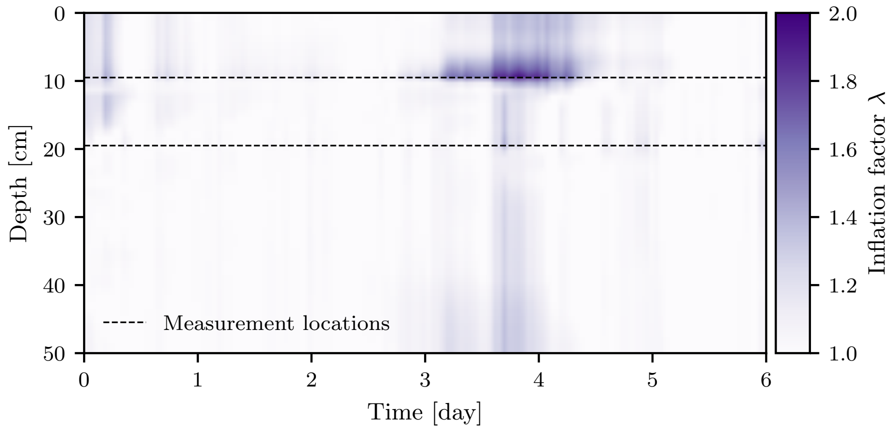


**Figure 2.** Inflation factor for the water content state. The inflation is strongest at the upper measurement location during the infiltration, when the uncertainty is underestimated the most. The inflation factor is transferred to the other measurement locations through the correlations in the Kalman gain. The used interpolation of Miller scaling factors impacts these correlations and leads to the smaller inflation directly below the measurement locations.

values. Accordingly, the inflation factor is increased quickly in the beginning and then reduced back to 1 when the estimation of $\log_{10}(\xi_1)$ reaches and eventually underestimates the true value. The underestimation of the scaling factor corresponds to a too fine material, which leads to slower changes in the water content state and therefore smaller correlations. The scaling factor is corrected during the rain event on the fourth day, which also leads to an inflation.

The initial guess for the scaling factor for the depth of 19.5 cm underestimates the scaling factor, which corresponds to a too fine material. Again, the correlations are small. The value increases slowly during the dry period in the beginning, but is inflated and adjusted strongly during the rain event.

The saturated hydraulic conductivity $K_0$ (Fig. 3(c)) was chosen to start a little more than one standard deviation below the true value. Due to the unrepresented heterogeneity in the beginning, the value decreases even further. The inflation remains very small due to correlations to both measurement locations. However, as soon as the infiltration event reaches the first measurement location, the value is corrected towards the true value. At the same time, the inflation factor is increased due to the too small uncertainty. After the rain event the inflation factor drops rapidly back to one. The hydraulic conductivity remains below the true value. Another rain event would be required to improve the estimation further.

The tortuosity $\tau$ (Fig. 3(d)) also influences the hydraulic conductivity function, but has in this case much smaller impact and consequently smaller correlations to the measurements than $K_0$. We use it as an indicator parameter and start at the true value. During the infiltration event the value is changed due to its correlation. The corresponding inflation factor is increased as well, but remains small enough and drops back to 1 quickly enough to not cause any over-inflation of the parameter.

To emphasize the need of a fast adapting inflation factor, we reduce the uncertainty of the inflation factors to ~~$\sigma^2_\lambda =$~~ $\sigma_\lambda =$ 0.5 to slow down their adjustment. The results are summarized in Fig. 4. The inflation of the water content state (Fig. 4(a)) shows,

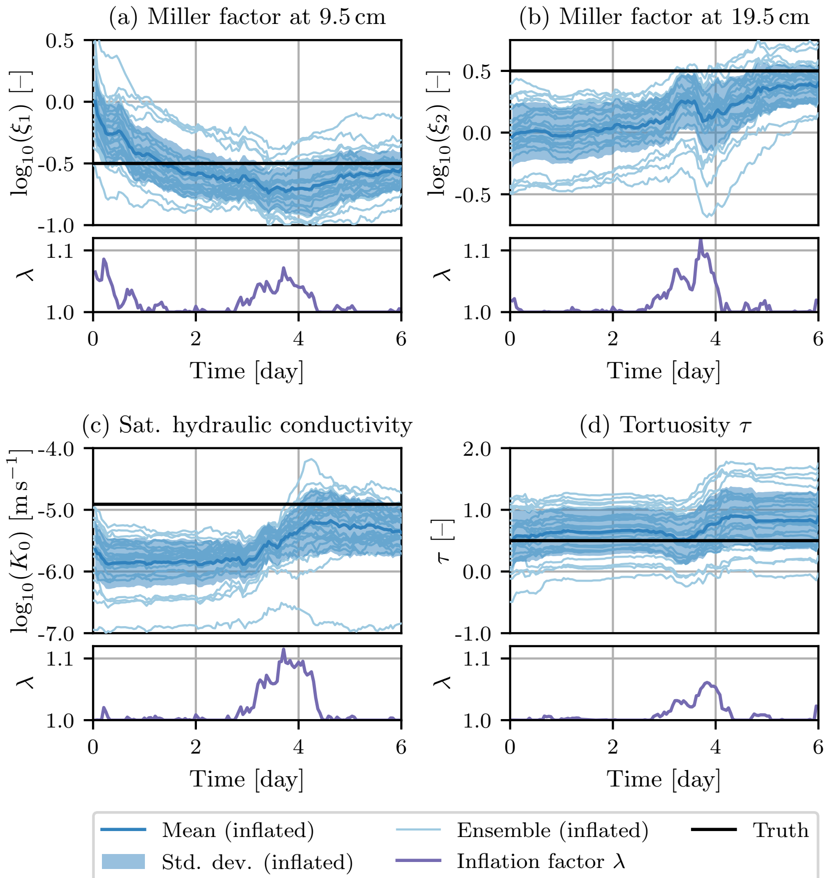


**Figure 3.** Development of Miller scaling factors $\xi_1$ and $\xi_2$, saturated hydraulic conductivity $K_0$ and tortuosity $\tau$ together with their corresponding inflation factors during estimation with the EnKF.

that the inflation factor does not reach as high values as before (see Fig. 2). To compensate for this, the inflation acts over a longer period of time. The same effect is also observed in the inflation of the parameters (Fig. 4(b) and (c)). This leads to a smaller inflation during the rain event and consequently a too small uncertainty. At later times, when the cause of the error is not active any more, the correlations to measurement locations are reduced leading to a slower reduction of the inflation in the parameters. In the indicator parameter $\tau$ the beginning of an over-inflation can be seen towards later times. This necessitates a more rapid inflation when correlations are used to update inflation information.

The results for the parameters $K_0$ and $\tau$ of a run without inflation (and only damping) are shown in Fig. 5. Again, $K_0$ moves further away from the true vale value due to the unrepresented heterogeneity and comes closer to the true value during the infiltration event. However, due to the wrong direction since the Miller scaling factor is not inflated in the beginning, the it is adjusted slower. Consequently, the $K_0$ is corrected longer in the wrong direction. The uncertainty eventually becomes too

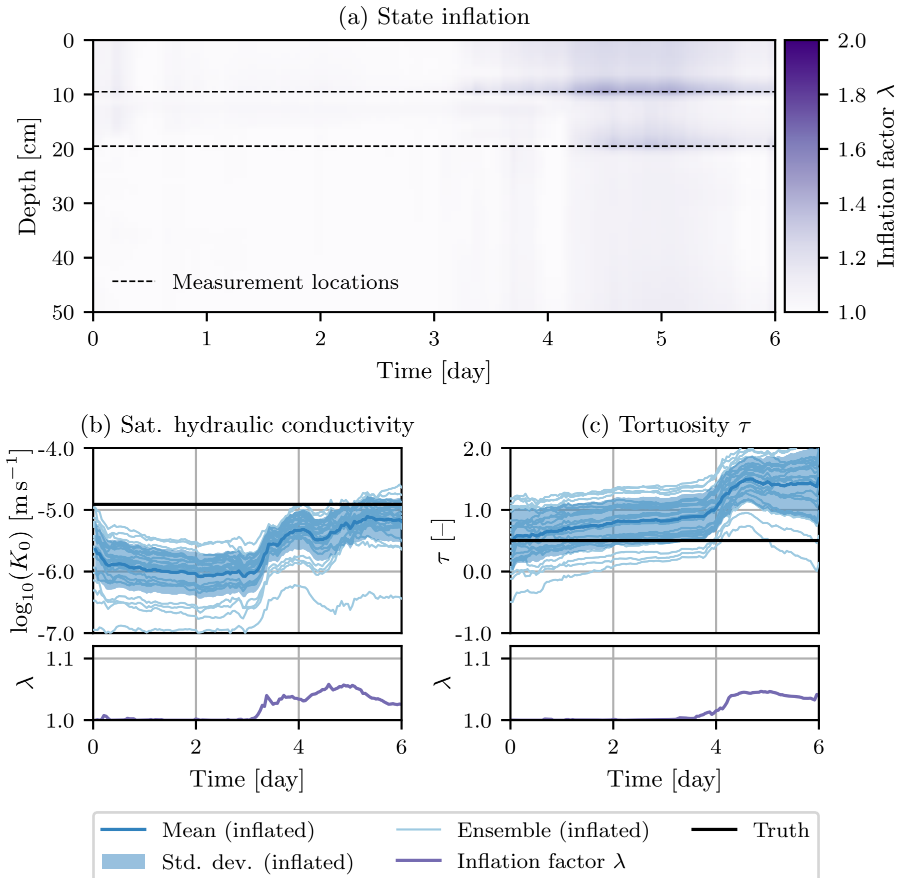


**Figure 4.** Development of the inflation factor for the water content state and saturated hydraulic conductivity $K_0$ and tortuosity $\tau$ together with their corresponding inflation factors for an estimation with a reduced inflation factor uncertainty of ~~$\sigma_\lambda^2 =$~~ $\sigma_\lambda =$ 0.5.

small and in the end the mean is ~~over~~ more than 5 standard deviations away from the true value, since the uncertainty cannot be increased any more.

As a side note: We have additionally tested the inflation method by reanalyzing the real-world application by Bauser et al. (2016), where measurements from 11 TDR probes were assimilated with an EnKF. There, the inflation method confirmed the behavior observed in the small synthetic case presented in this paper.

## 4 Discussion

The proposed inflation method uses a Kalman filter to estimate inflation factors within the EnKF. It is based on the difference between measurements and mean forecast state. It transfers correlations from the forecast of the augmented state to the inflation. Consequently, the performance will be limited if model errors are structurally not represented in the forecast error covariance

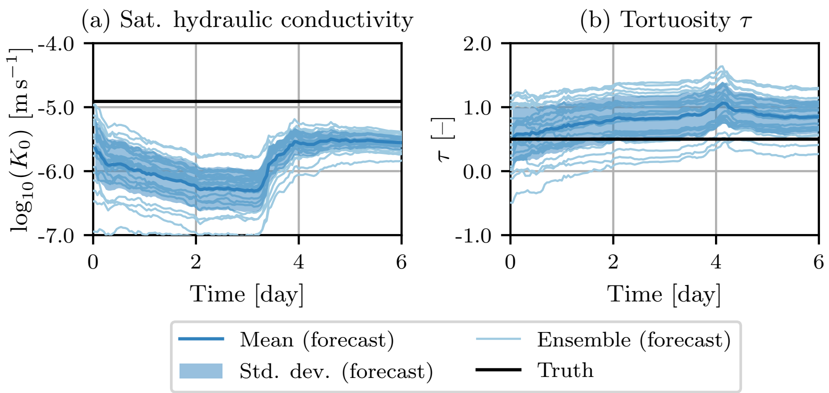


**Figure 5.** Development of saturated hydraulic conductivity $K_0$ and tortuosity $\tau$ for an estimation without inflation.

matrix. The estimation of the inflation factors with a Kalman Filter is, like the EnKF itself, based on a linearized analysis. The use of a damping factor can alleviate issues with estimating nonlinear dependent parameters. To keep the inflation consistent with the analysis in the EnKF, we apply the same damping factor for both.

We designed a small synthetic hydrologic test case for the inflation. This test case mimics a model error through initially unrepresented heterogeneity. We designed the test case so that a strong temporally varying inflation is necessary, as it can occur with real data. We choose a short time so that the details of the behavior of the method can be explored. The method showed that it is capable of inflating states and parameters. The inflation is adjusted fast and differentiates between parameters with strong and not so strong correlations. No over-inflation of weakly correlated parameters occurred. In this specific test case the estimation with inflation is far superior to an estimation without inflation.

The fast adjustment speed of the inflation factor is important because of the fast changing model errors and correlations to parameters. The adjustment speed is determined by the uncertainty of the inflation factor. This uncertainty is set to a constant value and has to be adjusted. For all our cases a value of ~~$\sigma^2_\lambda =$~~ $\sigma_\lambda =$ 1 was sufficient, but larger values were possible too. The need for such a fast adjustment is shown by estimating the same case with a reduced uncertainty of ~~$\sigma^2_\lambda =$~~ $\sigma_\lambda =$ 0.5, which leads to a slower adaptation of the inflation factor. This leads to smaller inflation factors, which is compensated by maintaining them for a longer period of time. In this test case this leads to inflation at times after the infiltration front has passed the measurements already and the model error is small again. This can cause over-inflation of weakly correlated parameters. Too large uncertainties of the inflation (in our test case $\sigma_\lambda = 4$), where the uncertainty is larger than the typical range for the values of lambda, can also lead to overinflation of weakly correlated parameters. Reasons for this can be the linearizations in the analysis and the calculation of the Jacobian (Eq. 14). This limits the adjustment speed of the inflation.

Fast dropping correlations between measurements and parameters are a limit for the method. An example could be a ~~multiplicative~~ parameter only acting on ~~the~~ an infiltration boundary condition. After the infiltration is over, correlations to this parameter would drop to zero and the inflation factor for this parameter will not be changed any more. If the inflation factor is not equal to 1 at this time, the parameter spread will keep increasing. In such a case, when there is no correlation, the parameter should be excluded from the estimation and consequently also from the inflation.

The method is in principle capable of compensating unrepresented model errors. However, this is limited to errors that can be represented with the it relies on correlations calculated from the forecast ensemble of the augmented state. If parameters are estimated along with the augmented state and have correlations to measurement locations with consistently underestimated forecast uncertainties, the inflation will keep increasing the parameter spread until the forecast uncertainties are increased sufficiently. This is the case when the Therefore the correlations have to contain useful information. This means that inflating the parameters based on their correlations to measurement locations has to increase the forecast spread at these measurement locations. If the parameters have an insufficient influence on the state uncertainty an over-inflation of the parameters can occur. An example are measurements with underestimated measurement uncertainties , when the dynamics is and short time between measurements compared to the timescale of the dynamics. Then the parameters are not able to follow the increase the state uncertainty in the short forecast time between measurements and the forecast dynamics is not able represent the measurement noise. If such errors occur intermittently, e.g., the closed-eye period as proposed by Bauser et al. (2016) could be used to bridge these times. A rather heuristic solution could be a decay of the inflation factor towards values of 1, as already proposed by Anderson (2009).

## 5 Conclusions

In this work we propose a novel spatiotemporally adaptive inflation method, specifically designed for soil hydrology, which nevertheless is expected to work in similar systems as well. The inflation method is based on a Kalman filter acting within the EnKF. The method is capable of rapid adjustments of inflation factors, treating each augmented state dimension individually. This rapid adjustment is required due to temporally varying model errors, as they can appear through violation of the local equilibrium assumption of the Richards equation, hysteresis, or unrepresented heterogeneity.

We demonstrate the use of our inflation method in combination with a damping factor on a small hydrologic example. We choose heterogeneity as a possible model error, but allow the heterogeneity to be estimated along with the soil hydrologic parameters $K_0$ and $\tau$ of the Mualem–van Genuchten parameterization. Our proposed inflation method proved to be stable in combination with parameter estimation. The performance of the estimation improved and parameter uncertainty remained consistent. The method requires , that model errors can be represented through the augmented statethat the correlations from in the forecast ensemble contain useful information for the inflation. However, we demonstrate that it even works for only weakly correlated parameters. We expect the inflation method to generally improve data assimilation with the EnKF and to thus lead to better state and parameter estimations in soil hydrology.

## Appendix A: Jacobian in the inflation method

We briefly show the derivation of the Jacobian matrix $\mathbf{H}_\lambda$ for the inflation (Eq. 14). Again, the entrywise product is denoted by $\circ$ and the entrywise square root of $\boldsymbol{\lambda}$ by $\sqrt{\boldsymbol{\lambda}}$:

$$
\begin{aligned}
(\mathbf{H}_\lambda)_{ij} &= \frac{\partial}{\partial\left(\boldsymbol{\lambda}^{\mathrm{f}}\right)_j}\left(\boldsymbol{h}_\lambda(\boldsymbol{\lambda}^{\mathrm{f}})\right)_i \\
&= \frac{\partial}{\partial(\boldsymbol{\lambda}^{\mathrm{f}})_j}\left[(\mathbf{R})_{ii} + \left(\mathbf{H}\left[\mathbf{P}^{\mathrm{f}}\circ\left[\sqrt{\boldsymbol{\lambda}^{\mathrm{f}}}\sqrt{\boldsymbol{\lambda}^{\mathrm{f}}}^T\right]\right]\mathbf{H}^T\right)_{ii}\right]^{\frac{1}{2}}, \text{ with } \mathbf{P}^{\mathrm{f}} \text{ symmetric} \\
&= \frac{\partial}{\partial(\boldsymbol{\lambda}^{\mathrm{f}})_j}\left[(\mathbf{R})_{ii} + \sum_m\sum_k(\mathbf{H})_{im}(\mathbf{H})_{ik}\left(\mathbf{P}^{\mathrm{f}}\right)_{km}\left[(\boldsymbol{\lambda}^{\mathrm{f}})_m\right]^{\frac{1}{2}}\left[(\boldsymbol{\lambda}^{\mathrm{f}})_k\right]^{\frac{1}{2}}\right]^{\frac{1}{2}} \\
&= \left[2\left(\boldsymbol{h}_\lambda(\boldsymbol{\lambda}^{\mathrm{f}})\right)_i\right]^{-1}\sum_m\sum_k(\mathbf{H})_{im}(\mathbf{H})_{ik}\left(\mathbf{P}^{\mathrm{f}}\right)_{km}\frac{\partial}{\partial(\boldsymbol{\lambda}^{\mathrm{f}})_j}\left[\left[(\boldsymbol{\lambda}^{\mathrm{f}})_m\right]^{\frac{1}{2}}\left[(\boldsymbol{\lambda}^{\mathrm{f}})_k\right]^{\frac{1}{2}}\right] \\
&= \left[2\left(\boldsymbol{h}_\lambda(\boldsymbol{\lambda}^{\mathrm{f}})\right)_i\right]^{-1}\sum_m\sum_k(\mathbf{H})_{im}(\mathbf{H})_{ik}\left(\mathbf{P}^{\mathrm{f}}\right)_{km}\frac{1}{2}\left[\delta_{mj}\frac{\left[(\boldsymbol{\lambda}^{\mathrm{f}})_k\right]^{\frac{1}{2}}}{\left[(\boldsymbol{\lambda}^{\mathrm{f}})_m\right]^{\frac{1}{2}}} + \delta_{kj}\frac{\left[(\boldsymbol{\lambda}^{\mathrm{f}})_m\right]^{\frac{1}{2}}}{\left[(\boldsymbol{\lambda}^{\mathrm{f}})_k\right]^{\frac{1}{2}}}\right] \\
&= \left[2\left[(\boldsymbol{\lambda}^{\mathrm{f}})_j\right]^{\frac{1}{2}}\left(\boldsymbol{h}_\lambda(\boldsymbol{\lambda}^{\mathrm{f}})\right)_i\right]^{-1}\sum_m(\mathbf{H})_{ij}(\mathbf{H})_{im}\left(\mathbf{P}^{\mathrm{f}}\right)_{jm}\left[(\boldsymbol{\lambda}^{\mathrm{f}})_m\right]^{\frac{1}{2}}.
\end{aligned}
\tag{A1}
$$

*Competing interests.* The authors declare that they have no conflict of interest.

*Acknowledgements.* This research is funded by Deutsche Forschungsgemeinschaft (DFG) through project RO 1080/12-1 and the Ministerium für Wissenschaft, Forschung und Kunst Baden-Württemberg (Az 33-7533.-30-20/6/2). HGS MathComp provided travel expenses for Hannes H. Bauser and Daniel Berg.

## References


Anderson, J. L.: An ensemble adjustment Kalman filter for data assimilation, Monthly Weather Review, 129, 2884–2903, https://doi.org/10.1175/1520-0493(2001)129<2884:AEAKFF>2.0.CO;2, 2001.

Anderson, J. L.: An adaptive covariance inflation error correction algorithm for ensemble filters, Tellus A, 59, 210–224, https://doi.org/10.1111/j.1600-0870.2006.00216.x, 2007.

Anderson, J. L.: Spatially and temporally varying adaptive covariance inflation for ensemble filters, Tellus A, 61, 72–83, https://doi.org/10.1111/j.1600-0870.2008.00361.x, 2009.

Anderson, J. L. and Anderson, S. L.: A Monte Carlo implementation of the nonlinear filtering problem to produce ensemble assimilations and forecasts, Monthly Weather Review, 127, 2741–2758, https://doi.org/10.1175/1520-0493(1999)127<2741:AMCIOT>2.0.CO;2, 1999.

Bateni, S. M. and Entekhabi, D.: Surface heat flux estimation with the ensemble Kalman smoother: Joint estimation of state and parameters, Water Resources Research, 48, https://doi.org/10.1029/2011WR011542, w08521, 2012.

Bauser, H. H., Jaumann, S., Berg, D., and Roth, K.: EnKF with closed-eye period – towards a consistent aggregation of information in soil hydrology, Hydrology and Earth System Sciences, 20, 4999–5014, https://doi.org/10.5194/hess-20-4999-2016, 2016.

Botto, A., Belluco, E., and Camporese, M.: Multi-source data assimilation for physically-based hydrological modeling of an experimental hillslope, Hydrology and Earth System Sciences Discussions, 2018, 1–26, https://doi.org/10.5194/hess-2018-18, 2018.

Brandhorst, N., Erdal, D., and Neuweiler, I.: Soil moisture prediction with the ensemble Kalman filter: Handling uncertainty of soil hydraulic parameters, Advances in Water Resources, 110, 360–370, https://doi.org/10.1016/j.advwatres.2017.10.022, 2017.

Burgers, G., van Leeuwen, P. J., and Evensen, G.: Analysis scheme in the ensemble Kalman filter, Monthly Weather Review, 126, 1719–1724, https://doi.org/10.1175/1520-0493(1998)126<1719:ASITEK>2.0.CO;2, 1998.

Camporese, M., Paniconi, C., Putti, M., and Salandin, P.: Ensemble Kalman filter data assimilation for a process-based catchment scale model of surface and subsurface flow, Water Resources Research, 45, https://doi.org/10.1029/2008WR007031, 2009.

Carsel, R. F. and Parrish, R. S.: Developing joint probability distributions of soil water retention characteristics, Water Resources Research, 24, 755–769, https://doi.org/10.1029/WR024i005p00755, 1988.

Chen, Y. and Zhang, D.: Data assimilation for transient flow in geologic formations via ensemble Kalman filter, Advances in Water Resources, 29, 1107–1122, https://doi.org/10.1016/j.advwatres.2005.09.007, 2006.

Crow, W. T. and Van Loon, E.: Impact of incorect model error assumptions on the sequential assimilation of remotely sensed surface soil moisture, Journal of Hydrometeorology, 7, 421–432, https://doi.org/10.1175/JHM499.1, 2006.

De Lannoy, G. J. M., Houser, P. R., Pauwels, V. R. N., and Verhoest, N. E. C.: State and bias estimation for soil moisture profiles by an ensemble Kalman filter: Effect of assimilation depth and frequency, Water Resources Research, 43, https://doi.org/10.1029/2006WR005100, w06401, 2007.

De Lannoy, G. J. M., Houser, P. R., Verhoest, N. E. C., and Pauwels, V. R. N.: Adaptive soil moisture profile filtering for horizontal information propagation in the independent column-based CLM2.0, Journal of Hydrometeorology, 10, 766–779, https://doi.org/10.1175/2008JHM1037.1, 2009.

Erdal, D. and Cirpka, O. A.: Joint inference of groundwater-recharge and hydraulic-conductivity fields from head data using the ensemble Kalman filter, Hydrology and Earth System Sciences, 20, 555–569, https://doi.org/10.5194/hess-20-555-2016, 2016.

Erdal, D., Neuweiler, I., and Wollschläger, U.: Using a bias aware EnKF to account for unresolved structure in an unsaturated zone model, Water Resources Research, 50, 132–147, https://doi.org/10.1002/2012WR013443, 2014.

Erdal, D., Rahman, M., and Neuweiler, I.: The importance of state transformations when using the ensemble Kalman filter for unsaturated flow modeling: Dealing with strong nonlinearities, Advances in Water Resources, 86, 354–365, https://doi.org/10.1016/j.advwatres.2015.09.008, 2015.

Evensen, G.: Sequential data assimilation with a nonlinear quasi-geostrophic model using Monte Carlo methods to forecast error statistics, Journal of Geophysical Research: Oceans, 99, 10 143–10 162, https://doi.org/10.1029/94JC00572, 1994.

Evensen, G.: The ensemble Kalman filter: theoretical formulation and practical implementation, Ocean Dynamics, 53, 343–367, https://doi.org/10.1007/s10236-003-0036-9, 2003.

Gaspari, G. and Cohn, S. E.: Construction of correlation functions in two and three dimensions, Quarterly Journal of the Royal Meteorological Society, 125, 723–757, https://doi.org/10.1002/qj.49712555417, 1999.

Hamill, T. M., Whitaker, J. S., and Snyder, C.: Distance-dependent filtering of background error covariance estimates in an ensemble Kalman filter, Monthly Weather Review, 129, 2776–2790, https://doi.org/10.1175/1520-0493(2001)129<2776:DDFOBE>2.0.CO;2, 2001.

Han, X., Franssen, H.-J. H., Montzka, C., and Vereecken, H.: Soil moisture and soil properties estimation in the Community Land Model with synthetic brightness temperature observations, Water Resources Research, 50, 6081–6105, https://doi.org/10.1002/2013WR014586, 2014.

Hendricks Franssen, H. J. and Kinzelbach, W.: Real-time groundwater flow modeling with the ensemble Kalman filter: Joint estimation of states and parameters and the filter inbreeding problem, Water Resources Research, 44, https://doi.org/10.1029/2007WR006505, w09408, 2008.

Ippisch, O., Vogel, H.-J., and Bastian, P.: Validity limits for the van Genuchten–Mualem model and implications for parameter estimation and numerical simulation, Advances in Water Resources, 29, 1780–1789, https://doi.org/10.1016/j.advwatres.2005.12.011, 2006.

Jaumann, S. and Roth, K.: Effect of unrepresented model errors on estimated soil hydraulic material properties, Hydrology and Earth System Sciences, 21, 4301–4322, https://doi.org/10.5194/hess-21-4301-2017, 2017.

Kalman, R. E.: A new approach to linear filtering and prediction problems, Journal of basic Engineering, 82, 35–45, 1960.

Kurtz, W., Hendricks Franssen, H.-J., and Vereecken, H.: Identification of time-variant river bed properties with the ensemble Kalman filter, Water Resources Research, 48, https://doi.org/10.1029/2011WR011743, w10534, 2012.

Kurtz, W., Hendricks Franssen, H.-J., Kaiser, H.-P., and Vereecken, H.: Joint assimilation of piezometric heads and groundwater temperatures for improved modeling of river-aquifer interactions, Water Resources Research, 50, 1665–1688, https://doi.org/10.1002/2013WR014823, 2014.

Li, C. and Ren, L.: Estimation of unsaturated soil hydraulic parameters using the ensemble Kalman filter, Vadose Zone Journal, 10, 1205–1227, https://doi.org/10.2136/vzj2010.0159, 2011.

Li, H., Kalnay, E., and Miyoshi, T.: Simultaneous estimation of covariance inflation and observation errors within an ensemble Kalman filter, Quarterly Journal of the Royal Meteorological Society, 135, 523–533, https://doi.org/10.1002/qj.371, 2009.

Liu, Y. and Gupta, H. V.: Uncertainty in hydrologic modeling: Toward an integrated data assimilation framework, Water Resources Research, 43, https://doi.org/10.1029/2006WR005756, w07401, 2007.

Liu, Y., Weerts, A. H., Clark, M., Hendricks Franssen, H.-J., Kumar, S., Moradkhani, H., Seo, D.-J., Schwanenberg, D., Smith, P., van Dijk, A. I. J. M., van Velzen, N., He, M., Lee, H., Noh, S. J., Rakovec, O., and Restrepo, P.: Advancing data assimilation in operational hydrologic forecasting: progresses, challenges, and emerging opportunities, Hydrology and Earth System Sciences, 16, 3863–3887, https://doi.org/10.5194/hess-16-3863-2012, 2012.

Miller, E. E. and Miller, R. D.: Physical theory for capillary flow phenomena, Journal of Applied Physics, 27, 324–332, https://doi.org/10.1063/1.1722370, 1956.

Moradkhani, H., Sorooshian, S., Gupta, H. V., and Houser, P. R.: Dual state–parameter estimation of hydrological models using ensemble Kalman filter, Advances in Water Resources, 28, 135–147, https://doi.org/10.1016/j.advwatres.2004.09.002, 2005.

Mualem, Y.: A new model for predicting the hydraulic conductivity of unsaturated porous media, Water Resources Research, 12, 513–522, https://doi.org/10.1029/WR012i003p00513, 1976.

Reichle, R. H.: Data assimilation methods in the Earth sciences, Advances in Water Resources, 31, 1411–1418, https://doi.org/10.1016/j.advwatres.2008.01.001, 2008.

Reichle, R. H., McLaughlin, D. B., and Entekhabi, D.: Hydrologic data assimilation with the ensemble Kalman filter, Monthly Weather Review, 130, 103–114, https://doi.org/10.1175/1520-0493(2002)130<0103:HDAWTE>2.0.CO;2, 2002.

Shi, L., Song, X., Tong, J., Zhu, Y., and Zhang, Q.: Impacts of different types of measurements on estimating unsaturated flow parameters, Journal of Hydrology, 524, 549–561, https://doi.org/10.1016/j.jhydrol.2015.01.078, 2015.

Song, X., Shi, L., Ye, M., Yang, J., and Navon, I. M.: Numerical comparison of iterative ensemble Kalman filters for unsaturated flow inverse modeling, Vadose Zone Journal, 13, https://doi.org/10.2136/vzj2013.05.0083, 2014.

van Genuchten, M. T.: A closed-form equation for predicting the hydraulic conductivity of unsaturated soils, Soil Science Society of America Journal, 44, 892–898, https://doi.org/10.2136/sssaj1980.03615995004400050002x, 1980.

van Leeuwen, P. J., Cheng, Y., and Reich, S.: Nonlinear data assimilation, vol. 2, Springer, https://doi.org/10.1007/978-3-319-18347-3, 2015.

Vereecken, H., Huisman, J. A., Hendricks Franssen, H. J., Brüggemann, N., Bogena, H. R., Kollet, S., Javaux, M., van der Kruk, J., and Vanderborght, J.: Soil hydrology: Recent methodological advances, challenges, and perspectives, Water Resources Research, 51, 2616–2633, https://doi.org/10.1002/2014WR016852, 2015.

Vrugt, J. A., Diks, C. G. H., Gupta, H. V., Bouten, W., and Verstraten, J. M.: Improved treatment of uncertainty in hydrologic modeling: Combining the strengths of global optimization and data assimilation, Water Resources Research, 41, https://doi.org/10.1029/2004WR003059, w01017, 2005.

Wang, X. and Bishop, C. H.: A Comparison of breeding and ensemble transform Kalman filter ensemble forecast schemes, Journal of the Atmospheric Sciences, 60, 1140–1158, https://doi.org/10.1175/1520-0469(2003)060<1140:ACOBAE>2.0.CO;2, 2003.

Whitaker, J. S. and Hamill, T. M.: Evaluating methods to account for system errors in ensemble data assimilation, Monthly Weather Review, 140, 3078–3089, https://doi.org/10.1175/MWR-D-11-00276.1, 2012.

Whitaker, J. S., Hamill, T. M., Wei, X., Song, Y., and Toth, Z.: Ensemble data assimilation with the NCEP global forecast system, Monthly Weather Review, 136, 463–482, https://doi.org/10.1175/2007MWR2018.1, 2008.

Wu, C.-C. and Margulis, S. A.: Feasibility of real-time soil state and flux characterization for wastewater reuse using an embedded sensor network data assimilation approach, Journal of Hydrology, 399, 313–325, https://doi.org/10.1016/j.jhydrol.2011.01.011, 2011.

Wu, C.-C. and Margulis, S. A.: Real-time soil moisture and salinity profile estimation using assimilation of embedded sensor datastreams, Vadose Zone Journal, 12, https://doi.org/10.2136/vzj2011.0176, 2013.

Ying, Y. and Zhang, F.: An adaptive covariance relaxation method for ensemble data assimilation, Quarterly Journal of the Royal Meteorological Society, 141, 2898–2906, https://doi.org/10.1002/qj.2576, 2015.

Zhang, F., Snyder, C., and Sun, J.: Impacts of initial estimate and observation availability on convective-scale data assimilation with an ensemble Kalman filter, Monthly Weather Review, 132, 1238–1253, https://doi.org/10.1175/1520-0493(2004)132<1238:IOIEAO>2.0.CO;2, 2004.

Zhang, H., Hendricks Franssen, H.-J., Han, X., Vrugt, J. A., and Vereecken, H.: State and parameter estimation of two land surface models using the ensemble Kalman filter and the particle filter, Hydrology and Earth System Sciences, 21, 4927–4958, https://doi.org/10.5194/hess-21-4927-2017, 2017.